Comparison of Methodologies Used to Determine Monolignol Ratios in Lignocellulosic Biomass

Renee M. Happs

National Renewable Energy Laboratory

Bennett Addison

National Renewable Energy Laboratory

Crissa Doeppke

National Renewable Energy Laboratory

Bryon S. Donohoe

National Renewable Energy Laboratory

Mark F. Davis

National Renewable Energy Laboratory

Anne Elizabeth Harman-Ware (✉ anne.ware@nrel.gov)

Renewable Resources and Enabling Sciences Center, National Renewable Energy Laboratory, Golden, CO 80401, USA   https://orcid.org/0000-0002-7927-9424

Abstract

Background

Multiple analytical methods have been developed to determine the ratios of monolignol monomers, particularly the syringyl/guaiacyl (S/G) ratio, of lignin biopolymers in plant cell walls. Chemical degradation methods yield monomers that are either selective of certain linkages, such as thioacidolysis, or induce chemical changes rendering it impossible to distinguish and determine the source of specific monomers, such as nitrobenzene oxidation. NMR methods provide powerful tools used to analyze cell walls for lignin monomeric composition and linkage information. Pyrolysis-mass spectrometry methods are also widely used, particularly as a high-throughput method. However, the different techniques used to analyze lignin monolignol ratios frequently yield different results within particular studies, making it difficult to interpret and compare results, and to obtain meaningful insights relating these measurements to other characteristics of plant cell walls that may impact biomass sustainability and conversion metrics for the production of bio-derived fuels and chemicals.

Results

The authors compared the S/G monolignol ratios of pine, several genotypes of poplar, and corn stover biomass obtained from thioacidolysis, pyrolysis-molecular beam mass spectrometry (py-MBMS), HSQC liquid-state NMR and solid-state (ss) NMR methodologies. An underutilized approach to deconvolute ssNMR spectra was implemented to derive S/G ratios. The S/G ratios obtained for the samples did not agree across the different methods, but trends were similar with the most agreement among the py-MBMS, HSQC NMR and deconvoluted ssNMR methods. The relationship between monolignol S/G, thioacidolysis yields, and linkage analysis determined by HSQC is also addressed.

Conclusions

This work demonstrates that different methods using chemical, thermal, and nondestructive NMR techniques to determine native monolignol S/G ratios in plant cell walls may yield different results depending on species and linkage abundances. Spectral deconvolution likely applies well to many hardwoods that are S and G dominant, but results may not be reliable for some woody and grassy species for which the lignin composition is more diverse. HSQC may be a better method for analyzing lignin in those species given the wealth of information provided on additional aromatic moieties and bond linkages. Careful consideration is required when choosing a method to measure S/G ratios and the benefits and shortcomings of each method discussed here are summarized.

Introduction

Lignin is an abundant aromatic polymer found in plant cell walls where it contributes to defense against insects and microbes, structural support of the plant, and water and nutrient transport [1]. Lignin is composed of aromatic units that vary in structure and composition depending on the plant species,

tissue type, and specific cell wall layer [2, 3]. The lignin content in hardwood tree species generally ranges from 18–30% of the dry wood mass and varies in the ratio of sinapyl or syringyl (S) phenylpropanoid monomers and coniferyl or guaiacyl (G) phenylpropanoid monomers while also consisting of a small amount of *p*-coumaryl (H) phenylpropanoid units. Softwood tree species such as pines consist of lignins that are predominantly composed of G monomers while grasses are composed of S, G, and H monomers and contain ferulates and coumarates in the cell walls. The S, G, and H canonical monolignols are typically the most abundant lignin monomers in most types of biomass but other non-conventional monomers such as caffeyl alcohol, tricin, resveratrol and others occur in certain types of biomass and tissues as reviewed in del Rio et al. [4].

In the context of developing technologies to use plant biomass as a source of renewable feedstock for fuels and chemicals, there has been significant interest in how lignin content and composition facilitates or inhibits access to cell wall carbohydrates by cellulolytic enzymes, and utilization of the lignin itself [5, 6]. Increased delignification rates of hardwoods have been shown to correlate with increases in S/G ratios [7]. Higher S content in woody species has also been correlated with greater pulping efficiency and higher lignin solubility [8, 9]. These results have been suggested to be due in part to the lower abundance of carbon-carbon linkages among S monomers relative to other monolignol moieties [10, 11]. Lignin content and S/G ratios could be critical biomass attributes in a biorefinery processes, particularly related to how these metrics impact enzymatic or acid hydrolysis of biomass to produce fermentable sugars [12–14]. The relative abundance of lignin monomers has also been shown to correlate with anaerobic digestion of biomass to produce methane [15]. Thus, by breeding or by directly engineering the lignin biosynthetic pathway in biomass species to give specific S/G ratios, biomass conversion to bioproducts and biofuels can be made more efficient and economical [16].

Various methods can be used to determine the relative abundance of lignin monomers, particularly the ratio of the most abundant S and G canonical monolignols (S/G ratio). Thioacidolysis is a common chemical degradation method used to quantitatively determine the S/G ratio of non-condensed lignin units in a variety of plant types [17, 18]. Thioacidolysis proceeds by cleaving β-O-4 ether linkages, where additional steps such as Raney nickel desulfurization, may be implemented to analyze dimers with C-C linkages [19, 20]. Variations in lignin structures across plant species lead to variations in monomer yields from thioacidolysis [17]. For example, the higher occurrence of C-C linkages involving the 5-position of G monomers in softwood lignins may negatively impact thioacidolysis monomer yields, while thioacidolysis monomer yields may be higher from hardwood lignins containing more S units (in comparison to softwoods) bound by ether linkages [18, 21]. Observations that higher S/G ratio lignins correspond to a more effective release of total monomers have been previously reported [22–27]. However, recent work has indicated that the S/G ratio of poplar as determined by thioacidolysis is not correlated to the yield of monomers produced by reductive catalytic fractionation (RCF), a thermochemical conversion technique relevant to lignin upgrading strategies or lignin characterization platforms [28].

Several spectroscopic methods have been developed to measure S/G ratios that attempt to circumvent the problems associated with chemical degradation of lignin. Methods that measure the S/G ratio by analyzing pyrolysis products give highly reproducible results; however, the measured S/G ratios do not always compare well with other degradative techniques [29−34]. Pyrolysis or thermal degradative methods coupled with chromatographic and/or mass spectrometry techniques can be performed on whole or minimally processed biomass and can be used in high-throughput platforms to analyze lignin content and composition in biomass [3, 35−39]. However, thermal degradation may overestimate the S content as products generated from labile ether linkages are detected whereas condensed linkages (either inherent or produced) may not be incorporated in the analyses, not unlike chemical degradation methods [40, 41].

[1]H and [13]C Nuclear Magnetic Resonance (NMR) spectroscopy, in both solution or gel and solid state, has also been widely used to study the structure and composition of lignin [42, 43]. Additionally, ^{31}P NMR has been employed as a method to investigate lignin structure by derivatization of phosphorus compounds to analyze hydroxyl groups in lignin subunits [44−46]. While this method provides advantages over ^{1}H and ^{13}C NMR, it requires extensive sample preparation and alteration of lignin as ^{31}P functional groups do not naturally occur in lignin, and it only analyzes solubilized components [47].

2D heteronuclear ([1]H-^{13}C) single quantum correlation (HSQC) spectroscopy is used to estimate S/G ratios from either isolated lignin or whole biomass among many different plant species, and alleviates some of the spectral overlap that occurs in 1D ^{1}H and ^{13}C methods; however, the method is not fully quantitative due to several parameters that are difficult to control in the experimental set-up [43, 48]. Whole cell wall analysis by NMR in a gel state can be performed by solubilizing biomass in various solvents, but these methods may suffer from incomplete solubilization, sample heterogeneity, and differences in relaxation times that can affect S/G ratio measurements [49−51]. Correction factors for 2D NMR methods used to quantitate monomer units have been proposed and give lower values than chemical degradation methods for hardwood species [52]. More recently, quantitative 2D NMR methods have been developed that addresses the relaxation problems associated with the previous methods in order to improve quantitation of monomer units [53]. The results from quantitative $HSQC_0$ have shown lower S/G ratios for *Miscanthus* than the previously reported ratios measured by thioacidolysis [53, 54]. More recently $HSQC_0$ has been employed to accurately predict depolymerization yields from lignin [55]. Generally, NMR methods in use today accommodate either isolated lignin or whole biomass for analysis [42].

A method to measure S/G ratios of hardwoods, without the need for degradation or extensive sample preparation, was developed by Manders et al. using ^{13}C solid-state NMR (ssNMR) [56] and versions of the method have been applied broadly [57−63]. The ^{13}C ssNMR method determines the S/G ratio by subtracting a softwood lignin spectrum (composed predominately of G monomers) from a hardwood spectrum. The obvious advantage of this approach comes from omitting the time-consuming lignin isolation step required in most chemical degradation methods, and many spectroscopic methods, which may lead to an enrichment of S units. However, the method developed by Manders assumes that the

softwood G-lignin ^{13}C ssNMR spectroscopic profile in the ~ 150 ppm range matches the G-lignin sub-profile of S- and G-rich hardwood, which may not be universally applicable across all biomass types [60]. As an alternative to the Manders method, spectral deconvolution of the aromatic region from quantitative or semi-quantitative ^{13}C ssNMR data has been used to obtain lignin composition [64–66].

The purpose of this manuscript is to compare the S/G ratios determined for a series of biomass samples including pine (softwood), poplar (hardwood), and corn stover (grass) as determined by thioacidolysis, py-MBMS, gel-state HSQC NMR, and ^{13}C ssNMR using spectral deconvolution peak fitting analysis to determine the relationships between analytical methodologies and the resulting monolignol ratios and linkages determined in different types of biomass. The novelty reported in this work is a comparison of 1) multiple deconstructive (py-MBMS and thioacidolysis) and non-destructive (solid-state NMR, gel-state HSQC NMR) analytical methods for determination of S/G ratios are compared in detail, 2) results from hardwood, softwood and grassy biomass sources to highlight strengths and weaknesses of each analytical, and 3) analysis of multiple samples from same plant type (poplar) were performed, which enabled a better comparison of characterization techniques over the natural lignin phenotypic range.

Results

Thioacidolysis

Thioacidolysis yields of lignin monomers for each of the biomass samples are presented in Table 1 (also Supplementary Table 1 with other S/G values determined by other methods). While the H monomer content determined by thioacidolysis was consistent among the set of poplar samples, the S and G monomer content varied widely, both in S/G ratio and total monomer yields. The S/G ratio determined by thioacidolysis did not correlate with the total yield of monomers (Pearson correlation = -0.08, Supplementary Table 2). However, the yield of S monomers was the primary driver in the total yield of thioethylated monomers for data both within poplar samples (Pearson correlation of S, total monomers = 0.92), Pearson correlation of G, total monomers = 0.62) and including the corn stover (Pearson correlation of S, total monomers = 0.94, Pearson correlation of G, total monomers = 0.68). Thioacidolysis of pine produced only G and H-derived monomers (ferulates and coumarates were not determined), similar to previously reported values [18]. The corn stover sample yielded lower total monomers from thioacidolysis than the hardwoods and softwood samples, which is typical for grasses [17, 18].

Table 1

Monomeric content of biomass determined by thioacidolysis (average of n = 2 samples, not all samples were analyzed by thioacidolysis and are denoted N/A).

Biomass ID	H µmol/g biomass	S µmol/g biomass	G µmol/g biomass	S/G	Sum µmol/g biomass
NIST 8493 Pine	6.7	0.0	205.7	-	217.7
FCIC Corn Stover	4.8	47.5	37.9	1.3	97.2
BESC-004 Poplar	5.5	218.5	105.6	2.1	329.6
BESC-021 Poplar	5.5	111.3	87.5	1.3	204.3
BESC-036 Poplar	5.4	207.3	69.4	3.0	282.0
BESC-075 Poplar	4.5	78.1	22.3	3.5	104.9
BESC-095 Poplar	N/A	N/A	N/A	N/A	N/A
BESC-096 Poplar	N/A	N/A	N/A	N/A	N/A
BESC-140 Poplar	5.0	156.3	40.7	4.0	202.0
BESC-169 Poplar	5.1	144.8	85.5	1.7	235.3
BESC-173 Poplar	N/A	N/A	N/A	N/A	N/A
BESC-182 Poplar	5.1	185.3	78.1	2.4	268.5
BESC-217 Poplar	5.1	147.0	57.3	2.6	209.4
BESC-219 Poplar	N/A	N/A	N/A	N/A	N/A
BESC-255 Poplar	N/A	N/A	N/A	N/A	N/A
BESC-282 Poplar	5.0	119.5	87.1	1.4	211.5
BESC-322 Poplar	N/A	N/A	N/A	N/A	N/A

Biomass ID	H μmol/g biomass	S μmol/g biomass	G μmol/g biomass	S/G	Sum μmol/g biomass
BESC-334 Poplar	5.0	198.1	68.4	2.9	271.6
BESC-388 Poplar	4.8	132.2	104.7	1.3	241.8
BESC-841 Poplar	5.1	231.4	68.3	3.4	304.8
BESC-853 Poplar	N/A	N/A	N/A	N/A	N/A
BESC-863 Poplar	4.8	138.6	62.9	2.2	206.3
BESC-883 Poplar	4.8	189.1	60.4	3.1	254.3

Py-MBMS

Py-MBMS of the biomass samples present in sufficient quantity (not all samples were analyzed) produced spectra consisting of ions derived from S, G, H, and other lignin monomers bound by various types of linkages. Lignin contents were determined based on methods described previously [35, 37, 38] in order to estimate Klason lignin content (wt %) using mean-normalized spectra to remove mass-dependent variation; S/G ratios were determined using unique (minimal-overlapping) ions of known origin that produced S/G ratios consistent with other methods in the literature [37, 67]. Therefore, traditional S/G ratios as determined by py-MBMS are covered in the context of being flexible where other ions may be considered as being derived from S, G, and H monomers based on the results from NMR and thioacidolysis.

Lignin content estimates of the poplar samples by py-MBMS ranged from 20.6 to 25.8 wt% lignin (Table 2). Traditional S/G ratios determined for the poplar samples using py-MBMS ranged from 1.3 to 2.2. Focusing on ions between 50–250 due to the nature of ions outside of that range originating primarily from noise and overlapping sources, the variance of the spectra was highest for m/z 138 (G lignin), 151 (G lignin, ferulate), 165 (S lignin), and 181 (S lignin), where () indicates origin of ion. The lignin content and S/G based on py-MBMS data were weakly correlated (Pearson correlation = 0.54) within the poplar samples. Lignin content as determined by py-MBMS did not strongly correlate with thioacidolysis yields for the entire poplar set either (Pearson correlation = 0.45, Supplementary Table 2). However, the majority of the poplar lignin estimates from py-MBMS did appear to correlate well with aromatic peaks from the peak-fit NMR data (values in Supplementary Table 1), although why some samples did not align would be speculative. The lignin content of the NIST 8493 Monterey pine was provided by the supplier based on Klason results to be 26.6 wt% lignin and the lignin content of the FCIC corn stover was estimated as 13.7 wt% relative to a corn stover sample of known Klason content using py-MBMS spectra. Table 2 provides characterization data of the biomass samples based on py-MBMS

analysis. The S/G ratio determined for the NIST pine was 0.2 since non-zero values of the ions otherwise derived from S-monomers were observed in the spectra, but these values could not be differentiated from noise and fragment ions and because pine does not produce S lignin the S/G for NIST pine was assigned to 0.

Table 2
Py-MBMS characterization of lignin content and monolignol ratios in select biomass samples (not all samples were analyzable by py-MBMS and are denoted N/A).

Biomass ID	S/G	Lignin content
NIST 8493 Pine	0.0*	26.6
FCIC Corn Stover	0.8	13.7
BESC-004 Poplar	1.9	25.8
BESC-021 Poplar	1.3	22.5
BESC-036 Poplar	2.1	24.4
BESC-075 Poplar	2.0	22.0
BESC-095 Poplar	N/A	N/A
BESC-096 Poplar	N/A	N/A
BESC-140 Poplar	2.0	24.2
BESC-169 Poplar	1.6	21.6
BESC-173 Poplar	N/A	N/A
BESC-182 Poplar	1.9	22.1
BESC-217 Poplar	2.0	23.6
BESC-219 Poplar	N/A	N/A
BESC-255 Poplar	N/A	N/A
BESC-282 Poplar	1.4	20.6
BESC-322 Poplar	N/A	N/A
BESC-334 Poplar	N/A	N/A
BESC-388 Poplar	1.4	21.4
BESC-841 Poplar	2.2	22.5
BESC-853 Poplar	N/A	N/A
BESC-863 Poplar	1.8	22.5
BESC-883 Poplar	2.1	23.6

*adjusted value based on S-derived lignin ion intensities low value

Gel state NMR (HSQC)

Gel-state HSQCs were collected on all poplar samples, as well as corn stover and pine, according to Mansfield et al. [51]. Generally, S/G ratios were consistent over triplicate runs, although the percent error ranged from as low as 2% to as high as 16%. It is believed that this range in error is partly due to inconsistencies in how well individual samples formed a gel. Some samples demonstrated better "gelling" after being heated to 40 °C for data collection, whereas other samples were unaffected (visual observation, data not shown). The S/G ratio of the corn stover and poplar samples ranged from 0.9 to 2.4. The S/G ratios of the poplar samples as determined by HSQC correlated strongly with the S/G ratios as determined by thioacidolysis (although the range for thioacidolysis was broader) and py-MBMS (Pearson correlation, HSQC/thioacidolysis = 0.84, HSQC/py-MBMS = 0.96, Supplementary Table 2).

Lignin monomeric linkages in the poplar samples as determined by HSQC provided structural information used to inform bias in methodologies used to measure S/G ratios. For example, β-O-4 linkages as determined by HSQC did not correlate with thioacidolysis yields (Pearson correlation = 0.11) and did not correlate strongly with lignin content as determined by py-MBMS (Pearson correlation = 0.45), indicating that the total yields of monomers as detected from thioacidolysis and by py-MBMS was not solely dependent on the abundance of those linkages in the biomass but is complicated by the other linkages as well. Additionally, the poplar β-O-4 linkages did not strongly correlate with S lignin monomer yields from thioacidolysis (Pearson correlation = 0.40) but did for py-MBMS ions typically derived from S lignins (Pearson correlation for most S-derived ions ~ 0.6, Supplementary Table 2). However, β-O-4 linkages in the poplar set did more strongly correlate with S/G ratio as determined by py-MBMS (Pearson correlation = 0.71), and to a lesser degree with S/G as determined by thioacidolysis (Pearson correlation = 0.70) and HSQC (Pearson correlation = 0.61). There was a general weakly negative correlation of poplar β-O-4 linkages with G monomers (Pearson correlation, HSQC/thioacidolysis = -0.51, HSQC/G monomers from py-MBMS ~ -0.5). Table 3 lists the calculated S/G and bond content results of triplicate analyses of poplar, pine, and corn stover samples.

Table 3
HSQC calculated S/G ratios and bond content.

Biomass ID	S/G Ratio	S/G Error	β-O-4	Error	β-β	Error	β-5	Error
NIST 8493 Pine	N/A	N/A	57	N/A	10	N/A	33	N/A
FCIC Corn Stover	1.1	0.20	99	N/A	N/A	N/A	N/A	N/A
BESC-004	1.6	0.15	70	2.0	24	1.4	6.1	1.2
BESC-021	0.89	0.04	66	2.6	25	2.4	9.4	1.5
BESC-036	1.9	0.17	74	3.8	21	4.1	4.8	2.1
BESC-075	2.1	0.05	72	2.3	23	2.1	4.6	0.4
BESC-095	1.5	0.21	75	2.6	20	1.2	5.2	2.4
BESC-096	2.1	0.25	76	2.3	20	2	3.4	0.9
BESC-140	1.7	0.11	74	4.2	22	2.8	4.3	1.5
BESC-169	1.2	0.05	73	1.9	21	0.5	6.5	2.1
BESC-173	1.1	0.13	69	2.1	23	1.1	8.2	1.0
BESC-182	1.8	0.20	73	4.1	21	3.7	5.9	2.3
BESC-217	1.7	0.18	72	0.5	23	2.1	5.3	1.8
BESC-219	2.3	0.13	72	1.8	25	3.1	2.8	1.6
BESC-255	1.8	0.17	71	3.4	22	3.0	6.2	1.0
BESC-282	1.1	0.04	62	3.7	25	2.6	14	4.8
BESC-322	2.2	0.19	75	2.4	22	1.9	3.2	0.8
BESC-334	2.3	0.21	69	2.3	27	1.4	4.5	1.0
BESC-388	0.94	0.01	67	4.4	22	2.4	11	3.1
BESC-841	2.4	0.30	73	5.7	23	5.9	3.8	1.8
BESC-853	2.4	0.33	73	3.8	23	1.6	3.3	2.4
BESC-863	1.4	0.12	73	4.3	23	2.9	4.1	1.7
BESC-883	2.3	0.36	76	1.8	21	2.9	2.5	1.4

Solid-State NMR – Manders Subtraction Method

The S/G ratios of poplar samples were calculated from solid-state ^{13}C NMR interrupted decoupling spectra as described by Manders [56]. Table 4 gives the integral values and the S/G ratios calculated using the Manders method for the poplar samples. A low, mid-range, and two high S/G ratio samples (as

calculated by py-MBMS) were run in triplicate to determine consistency of the Manders method. Generally, S/G ratios were consistent over triplicate runs, with the percent error ranging from 4−7%. Overall, the S/G ratios calculated trend much lower than all the other methods studied thus far and had a significantly lower range of S/G ratios. The S/G ratio of the corn stover and poplar samples ranged from 0.5 to 1.1. The S/G ratios of the poplar samples as determined by ssNMR still did correlate with the S/G ratios as determined by thioacidolysis, py-MBMS or HSQC (Pearson correlation, ssNMR/thioacidolysis = 0.76, ssNMR/py-MBMS = 0.81, ssNMR/HSQC = 0.80).

Table 4
Integration values of interrupted decoupling ssNMR spectra (Manders method)

Biomass ID	S Integral	G Integral	Normalized S	Normalized G	S/G
NIST 8493 Pine	N/A	100.0	N/A	33.3	N/A
FCIC Corn Stover	37.6	62.4	9.4	20.8	0.5
BESC-004	48.1	51.9	12.0	17.3	0.7
BESC-021*	46.4	53.6	11.6	17.9	0.7
BESC-036	52.3	47.7	13.1	15.9	0.8
BESC-075	53.2	46.8	13.3	15.6	0.9
BESC-095	52.8	47.2	13.2	15.7	0.8
BESC-096	59.2	40.8	14.8	13.6	1.1
BESC-140	54.8	45.2	13.7	15.1	0.9
BESC-169	43.7	56.3	10.9	18.8	0.6
BESC-173	47.5	52.5	11.9	17.5	0.7
BESC-182*	48.8	51.2	12.2	17.1	0.7
BESC-217	54.0	46.0	13.5	15.3	0.9
BESC-219	59.0	41.0	14.7	13.7	1.1
BESC-255	53.4	46.6	13.4	15.5	0.9
BESC-282	43.1	56.9	10.8	19.0	0.6
BESC-322	50.9	49.1	12.7	16.4	0.8
BESC-334	59.8	40.2	15.0	13.4	1.1
BESC-388*	45.7	54.3	11.4	18.1	0.6
BESC-841	54.6	45.4	13.7	15.1	0.9
BESC-853*	55.8	44.2	14.0	14.7	0.9
BESC-863	50.1	49.9	12.5	16.6	0.8
BESC-883	59.7	40.3	14.9	13.4	1.1

* Average of duplicate or triplicate sample runs

Solid-state NMR – Spectral Deconvolution

Spectral deconvolution (peak-fitting) of ^{13}C CP-MAS spectra in the aromatic domain was performed to estimate the relative abundances of S and G and lignin for twenty-two natural poplar variants and one

corn stover sample. Peak-fitting ^{13}C solid-state NMR data to quantitatively understand local molecular structure of biopolymers is a widely used practice, with many applications to biomass and other heterogeneous polymers [66, 68, 69]. Solid-state NMR profiles are generally deconvoluted into pseudo-Voight lineshapes, meaning a weighted sum of Gaussian and Lorentzian profiles are used for a single resonance. This means any particular ^{13}C NMR resonance has variables in peak position, amplitude, width (Full Width Half Max, or FWHM), and finally peak shape (Gaussian vs Lorentzian weighting factor). When deconvoluting overlapping resonances, inaccurate initial estimates of peak position, linewidth and peak shape might result in unreliable and inaccurate fits.

Therefore, to identify acceptable initial fitting conditions prior to spectral deconvolution, we collected 2D ^{13}C-^{13}C through-space Dipolar Assisted Rotational Resonance (DARR) spectra on model ^{13}C-enriched woody biomass (Fig. 1). Precise ^{13}C chemical shifts were extracted from inspection of off-diagonal cross-peaks, and reasonable linewidth estimates were obtained from analysis of resolved cross-peaks. S-lignin peaks were identified from S-lignin rich ^{13}C-enriched hybrid poplar woody stems (Fig. 1a), while G-lignin shifts were extracted from ^{13}C-enriched Monterey pine since softwood biomass is entirely G-lignin (Fig. 1b). We note that two signals centered at 146.5 and 148.5 could be identified in the 2D spectrum, which we use to generally represent $G_{3,4}$ moieties. Since guaiacyl monomers lack a methoxy group at the ring-5 position and are therefore subject to carbon-carbon and carbon-oxygen condensation, a broader distribution of chemical environments is expected for G units compared to the more symmetric S units. Minor G-lignin chemical shifts in the poplar biomass were consistent with G-lignin signals in the Pine sample. Peak shapes were initially set to mixed 90% Gaussian 10% Lorentzian component, because sample heterogeneity will impart a gaussian distribution of Lorentzian-like signals, although this weighting factor was varied systematically (from 9:1 to 1:9) to help identify fitting errors. To improve these initial starting parameters, a single CP-MAS spectrum representative of the full dataset was deconvoluted such that chemical shifts were only allowed to perturb by 0.1 ppm about the shifts identified from the 2D data, and peak widths and lineshapes were allowed minor deviation from initial guesses to obtain optimal fits. Finally, with initial chemical shifts, peak widths and peak shapes all carefully estimated, batch-fitting of the entire dataset was accomplished using Python code (fitting performed with lmfit module) in which only peak amplitude was allowed to vary for each spectrum whereas peak position, Gaussian/Lorentzian ratios and FWHM were locked for all samples. Representations of resulting spectral deconvolutions for High-S (BESC-096) and Low-S (BESC-021) lignin natural poplar variants are shown in Fig. 2. S/G ratios arise directly from the relative deconvoluted peak areas of the $S_{3,5}$ to $G_{3,4}$ signals.

When applying this fitting strategy, it became clear that small variations in the initial starting conditions had minor effects on the final observable, namely S/G ratios based on the 153/148 ppm peak areas. Since estimation of initial fitting parameters were obtained with a manual process and are therefore subject to some researcher bias, the above procedure was repeated several times. Table 5 lists are average S/G ratios obtained from repeated batch-fitting of the entire poplar and corn stover dataset using a range of different starting conditions.

Table 5
S/G ratios obtained from peak fitting for deconvolution of ssNMR (n = 7 fitting iterations).

Biomass ID	Average S/G	Std Dev
FCIC Corn Stover	0.74*	0.04
BESC-004	1.6	0.1
BESC-021	1.2	0.1
BESC-036	2.0	0.2
BESC-075	2.1	0.2
BESC-095	1.7	0.1
BESC-096	2.0	0.2
BESC-140	1.9	0.2
BESC-169	1.4	0.1
BESC-173	1.4	0.1
BESC-182	1.7	0.1
BESC-217	1.9	0.1
BESC-219	2.1	0.2
BESC-255	2.1	0.2
BESC-282	1.3	0.1
BESC-322	2.2	0.2
BESC-334	2.2	0.2
BESC-388	1.4	0.1
BESC-841	2.1	0.2
BESC-853	2.1	0.2
BESC-863	1.6	0.1
BESC-883	2.2	0.2
* Ratio measured = S/(G + FA)		

Discussion

Limitations, considerations, and the impact of cell wall structure on S/G and associated methodologies

A comparison of S/G ratios determined by four different methods for the poplar biomass analyzed is provided in Fig. 3 and Supplementary Table 1. Generally, thioacidolysis analyses resulted in higher S/G ratios and the Manders ssNMR method plateaued at 1.1, whereas HSQC and py-MBMS data yielded the most similar S/G ratios for the poplar and corn stover samples. The deconvoluted ssNMR spectra provided S/G measurement improvements over the Manders method to more carefully reflect S/G values determined by HSQC and py-MBMS.

Lignin is not evenly distributed within a plant. Past studies have shown that almost 75% of the lignin in hardwood is contained within fiber cells, containing predominately S type lignin, and only 25% of lignin is contained in vessel and ray cells [70]. Lignin concentration is also highest in the middle lamella of the fiber cells, but the secondary cell wall contains a higher concentration of S monomers [21, 71]. High concentrations of G units are present in the middle lamella, which may be more condensed, containing a higher proportion of the total C-C linkages present that would not be released during thioacidolysis. Since S type lignin tends to be dominant in the thicker, less dense secondary cell wall and would contain more β-O-4 linkages than G units, S units could be released more effectively. Overall, monomers, and therefore condensed structures, are not evenly distributed among plant tissue types or across cell wall layers. One can reasonably assume that G monomers may not be effectively released even at low S/G ratios. This could explain why the S/G ratio measured by thioacidolysis trends high, agreeing with previous observations regarding chemical degradation methods [23, 25, 27].

Similarly, since py-MBMS is only capable of releasing and detecting lignin monomers and dimers after breaking thermally labile linkages, it may also be biased towards the analysis of moieties bound by β-O-4 linkages, particularly S-lignin monomers. If S/G ratios measured by py-MBMS were heavily biased, impacted, or correlated with β-O-4 linkages, in addition to being positively correlated with S content, then the total lignin content estimated would also be influenced such that the higher lignin content would trend with S/G. Here, the lignin content of the poplar or entire biomass sets determined by py-MBMS did not correlate strongly with S/G and lignin content estimates did not correlate strongly with thioacidolysis yields. Therefore, and in addition to strong correlation with HSQC S/G which may be less biased although is otherwise only semi-quantitative, py-MBMS S/G determined by the traditional method could be an accurate representation of S/G ratios in biomass, pending other linkage or monomeric anomalies not explored here that may otherwise impact the data. However, given the relatively small sample size of this data set and since the lignin values determined by py-MBMS did not all consistently align with solid state aromatic NMR spectral features, it may be necessary to interpret some of these correlations with caution.

Several factors contribute to the error associated with the S/G ratios measured by ^{1}H-^{13}C HSQC volume integrations. HSQC experiments are generally not quantitative due to the way the experiment is typically performed. Cross-peaks in a ^{1}H-^{13}C HSQC experiment arise from polarization transfer through one-bond

J-coupling to correlate protons directly bonded to a carbon. While this provides tremendous information qualitatively, the intensity of the cross peaks is impacted by both heteronuclear and homonuclear coupling constants as well as T_1 and T_2 relaxation. A single ^{1}H-^{13}C HSQC experiment is generally optimized for one ^{1}H-^{13}C coupling constant; usually an average value of 145 Hz is chosen to capture both aromatic (~ 160 Hz) and aliphatic (~ 120 Hz) environments in an effort to optimize the number and intensity of the observed cross peaks. Additionally, relaxation is not accounted for in the same way as 1D experiments, where a delay of 5 x T_1 is employed. These delays make an HSQC experiment untenably long. The compounding effects of differing coupling constants and relaxation rates makes the cross-peak intensities for the poplar studied here semi-quantitative, meaning only relative amounts of lignin units or linkages can be compared between samples.

^{13}C ssNMR analysis of lignocellulosic biomass cell walls

Solid-state NMR data were processed in two different ways (Manders et al. and spectral deconvolution or peak fitting) to extract S/G estimates directly from the in-tact biomass. Results from both data processing methods trend correctly, but it appears the Manders subtraction method undercounts S/G ratio compared to spectral deconvolution. Like thioacidolysis, py-MBMS, and gel-state HSQC analyses, there are issues related to analyses of S/G by solid-state ^{13}C NMR methods. First, broad overlapping lines and overall poor resolution of 1D ^{13}C solid-state NMR data poses inherent challenges, especially if detailed analyses of lignin composition are desired. Second, due to the low sensitivity of NMR in general, compounded with the low (1.1%) natural abundance of ^{13}C, a single CP-MAS experiment usually requires long acquisition times. Sample throughput cannot possibly compete with some other analytical techniques used to obtain S/G estimates. Additionally, it is widely known that routine cross polarization NMR data is not inherently quantitative. In addition to experimental choices like magnetic field strength and rotor spinning speed, differences in cross polarization rates (T_{CH}), spin lattice relaxation times (T_1), and spin lattice relaxation times in the rotating frame ($T_{1\rho}$) for carbons in different chemical environments can affect their relative intensities [72, 73]. However, in our experiments, differences in CP rates can be neglected because 1) we operated at a reasonably low (50 MHz) ^{13}C Lamour frequency and low (6900 Hz) spinning speed such that the CP condition was quite robust, and 2) the S- and G-lignin carbons of interest used for analysis (respectively at 153 and 148 ppm) are both are non-protonated quaternary aromatic carbons in similar dynamic environments. In support, identical correction factors to adjust for variations in cross-polarization kinetics were found by Davis et al. for these two signals, confirming this assessment [64]. Therefore, careful experimental set up and data analysis can ensure that reproducible S/G ratios are determined counting all S and G units using the solid-state ^{13}C NMR method. That said, researchers operating at higher magnetic fields and faster spinning speeds may need to take more precautions.

It is clear from comparing S/G ratios determined using the Manders method with spectral deconvolution that the procedure in which the data is processed can significantly impact results. To explain the difference, we hypothesize that the method proposed by Manders of subtracting out the softwood-derived

G-lignin profile from S- and G-rich hardwood spectrum is somewhat flawed. As can be seen in Fig. 1b, in softwoods there exists a minor downfield shoulder in the G-lignin spectrum near 153 ppm. Based on multiple reports in the literature[67, 74–77] this signal can be assigned to G-lignin ring carbons at the 3, 4 and even 5 position depending on if the guaiacyl unit is or is not etherified, type of inter-unit linkage present and if carbon-oxygen condensation has occurred at the C5 position (labeled $G'_{3,4,5}$ in Fig. 1b). The abundance of the G-lignin downfield shoulder near 153 ppm seen in pure-G softwoods is therefore unlikely to match the same G-lignin profile in S- and G-rich hardwoods. As a result, subtracting a G-lignin profile from hardwood ^{13}C data could unintentionally subtract signal that is truly from S-lignin. This likely explains why S/G ratios obtained using the Manders method tend to under-represent syringyl units, while deconvolution of the same data produce S/G ratios that are consistent with HSQC and py-MBMS methods.

While promising, spectral deconvolution of ^{13}C ssNMR data may not be broadly applicable to all biomass types. Lignin from hardwoods is predominantly S and G with minor H monomeric subunits, *p*-hydroxybenzoates, ferulates (FA) and *p*-coumarate (pCA). Therefore, the aromatic region of the ^{13}C NMR spectrum of hardwoods like poplar is reasonably simple making spectral deconvolution straightforward. Corn stover, on the other hand, is known to be rich in S, G and H lignin monomers with an abundance of hydroxycinnamates such as FA and (pCA) levels. The S/G ratios determined from deconvolution of the 148–153 ppm region therefore likely overestimate guaiacyl content since FA and pCA moieties have spectral features near 147 ppm. Similarly, some biomass types have significant representations of non-conventional lignin monomers derived from flavonoids (tricin), hydroxystilbenes, and monolignol acetates [4]. In other words, the spectral deconvolution approach demonstrated here applied to poplar may work to characterize a specific type of biomass (hardwoods are particularly promising) but care must be taken when applying across biomass types. This concept is highlighted in our attempt to deconvolute ^{13}C ssNMR spectrum from corn stover. A ratio between the 153 and 147 ppm regions of 0.7 to 0.8 was observed similar to py-MBMS (0.8), but this does not match the S/G ratio of 1.1 measured from HSQC integrations or 1.3 as measured by thioacidolysis (Fig. 3). When FA content is considered, the S/(G + FA) ratios obtained from HSQC integrations (0.7, data not shown) and solid-state NMR peak-fitting analysis are consistent, confirming that G and FA content cannot be separately quantified in CP-MAS data.

Despite these limitations, solid-state NMR methods are powerful for biomass characterization because they are rich in structural information and data is obtained on samples in their native and unaltered states. For example, in addition to S/G ratios shown here, estimates for cellulose crystallinity index and lignin composition are accessible from the same CP-MAS data [78–80].

In choosing a methodology for studying lignin and particularly if evaluation of S/G ratios is required, the first criteria to consider is size of the sample set. Large sample sets where reliable high-throughput data is required are suitable for py-MBMS or potentially HSQC, but not for thioacidolysis or ssNMR methods. Additionally, if information beyond S/G ratios are required, HSQC spectra can provide bond linkage

information as well as other aromatic moieties present in lignin which becomes important for grassy species that are high in coumarates, ferulates and even H-type (p-hydroxyphenyl) lignin. Additionally, py-MBMS could also provide lignin content estimates or thioacidolysis total monomer yields may also be suitable methods if those metrics are needed, although it should be noted that thioacidolysis has the distinct limitation of only cleaving β-O-4 bonds and data will be biased accordingly. Py-MBMS should only compare lignin content of similar biomass types as well and comparing S/G across biomass types by py-MBMS may need to be interpreted with caution as well. If amount of sample is limited, then non-destructive methods may offer the best alternative, although care needs be taken when employing spectral deconvolution to estimate S/G ratios and it is recommended for use only by those with experience in spectral deconvolution. Both HSQC and ssNMR provide a look at intact cell walls, and while it could be argued that the ball-milling required for HSQC may affect cell wall structure, it is likely negligible so long as overheating is prevented and samples being compared are milled consistently. Table 6 summarizes the main considerations for each methodology reported here.

Table 6
Benefits and shortcomings associated with methods used for S/G analysis reported in this work.

Method	Benefit	Shortcoming
Thioacidolysis	Small sample size, high reproducibility, wealth of historical data	Potential bias for monomers released by β-O-4 linkages not being representative, sensitive to other components in biomass impacting reaction, laborious sample preparation
Py-MBMS	Small sample size, rapid analysis, high reproducibility, multiple cell wall phenotype measurements possible	Destructive, requires comparison within species, potential bias for monomers released by thermally labile linkages, semi-quantitative
^{1}H-^{13}C HSQC	Representative of whole cell wall, multiple cell wall phenotype measurements possible particularly including lignin linkage information	Semi-quantitative, large sample size requirement, long analysis time
ssNMR Manders	Non-Destructive	Underestimates contribution from S lignin monomers
ssNMR Deconvolution	Non-destructive, Representative of whole cell wall, multiple cell wall phenotype measurements possible	Low throughput, sensitive to incorrect initial peak-fitting parameters, not appropriate for grass species, need other *a priori* data

Conclusions

The analysis of S/G ratios of lignin in biomass from different poplar phenotypes, corn stover and Monterey pine samples were reported from different methods including thioacidolysis, py-MBMS, gel-state ^{1}H-^{13}C HSQC, and ssNMR using two different data analysis approaches - the Manders method and spectral deconvolution. Each method explored here has benefits and shortcomings for analyzing

monolignol components in biomass. If S/G ratios are being compared within species (for example, different phenotypes of poplar), methods such as HSQC, ^{13}C deconvoluted/peak fit ssNMR and py-MBMS, and thioacidolysis may provide sufficient, representative, comprehensive, and accurate information for lignin analysis studies. ^{13}C ssNMR deconvolution method for S/G analysis may not provide an accurate analysis for grass species. Comparing S/G across species (for example, grasses and hardwoods) may best be interpreted using HSQC data to take in context the lignin linkage information also captured. S/G comparisons across species are also traditionally performed using thioacidolysis and py-MBMS but if lignin linkages differ substantially, bias in S/G may be captured using these methods. In summary, methods used to analyze S/G in biomass could be impacted by lignin linkage structures. The methods used for comparing the S/G ratios determined within and across different types of biomass should be carefully considered in the context of the limitations of the methods and their resulting findings relationships with other lignin structural or linkage features.

Methods And Materials

Biomass

Populus trichocarpa biomass was grown as outlined in Table 7 and samples were dried and debarked, milled, destarched and extracted with ethanol/water prior to analysis [39]. Corn stover was harvested and baled in October 2017 in Story County, Iowa. Bales were stored field-side for 2 months until being transported and placed in covered storage. A *Pinus radiata* (Monterey pine) sample used to represent a predominately guaiacyl-based lignin was obtained from the National Institute of Standards and Technology (NIST). ^{13}C-enriched hardwood (DN34 poplar) and softwood (*Pinus radiata*, Monterey Pine, IsoLife) samples were also used to inform spectral deconvolution method development. Samples were extracted in a Soxhlet extractor using an ethanol solution and then dried under vacuum for 12 hours.

Table 7

Samples used for lignin analysis. Samples were chosen based on a range of phenotypes including S/G ratios as determined by py-MBMS.

Sample	Biomass Species	Source
Pine	*Pinus radiata* (Monterey Pine)	NIST standard 8493
^{13}C-enriched pine	*Pinus radiata* (Monterey Pine)	IsoLife
FCIC Corn stover	*Zea mays*	Iowa, USA
BESC-021	*Populus trichocarpa*	Pacific Northwest, USA
BESC-036	*Populus trichocarpa*	Pacific Northwest, USA
BESC-075	*Populus trichocarpa*	Pacific Northwest, USA
BESC-095	*Populus trichocarpa*	Pacific Northwest, USA
BESC-096	*Populus trichocarpa*	Pacific Northwest, USA
BESC-140	*Populus trichocarpa*	Pacific Northwest, USA
BESC-169	*Populus trichocarpa*	Pacific Northwest, USA
BESC-173	*Populus trichocarpa*	Pacific Northwest, USA
BESC-182	*Populus trichocarpa*	Pacific Northwest, USA
BESC-217	*Populus trichocarpa*	Pacific Northwest, USA
BESC-219	*Populus trichocarpa*	Pacific Northwest, USA
BESC-255	*Populus trichocarpa*	Pacific Northwest, USA
BESC-282	*Populus trichocarpa*	Pacific Northwest, USA
BESC-322	*Populus trichocarpa*	Pacific Northwest, USA
BESC-334	*Populus trichocarpa*	Pacific Northwest, USA
BESC-388	*Populus trichocarpa*	Pacific Northwest, USA
BESC-841	*Populus trichocarpa*	Pacific Northwest, USA
BESC-853	*Populus trichocarpa*	Pacific Northwest, USA
BESC-863	*Populus trichocarpa*	Pacific Northwest, USA
BESC-883	*Populus trichocarpa*	Pacific Northwest, USA

Thioacidolysis

Thioacidolysis was performed on 2 mg of ground sample that was previously destarched and extracted, as reported in Harman-Ware et al. [18]. Samples were analyzed and yields were quantified by GC/MS

using internal standard response factors built from external calibration standards of synthesized monolignol H, G and S arylglycerol species as reported in [81].

Py-MBMS

Approximately 4 mg of ground biomass samples were pyrolyzed using a Frontier PY2020 unit at 500°C for 30 s in 80 µL deactivated stainless steel cups and analyzed in duplicate. Mass spectral data was acquired using an Extrel Super-Sonic MBMS Model Max 1000 and processed using Merlin Automation software (V3). Spectra were collected from *m/z* 30 to 450 at 17 eV. Lignin content was estimated in poplar sample set relative to NIST standard 8492 *Populus deltoides* of known Klason lignin content and corn stover lignin content was estimated relative to a reference corn stover material of known Klason lignin content. Ion intensities *m/z* 120, 124 (G), 137 (G), 138 (G), 150 (G), 152, 154 (S), 164 (G), 167 (S), 168 (S), 178 (G), 180, 181, 182 (S), 194 (S), 208 (S) and 210 (S) where G denotes primarily guaiacyl-derived ions, S denotes primarily syringyl-derived ions, where other ions derived from other lignin monomers or multiple sources, were mean-normalized and summed to obtain relative lignin contents. Monolignol syringyl to guaiacyl (S/G) ratios were determined by dividing the sum of S-based ions by the sum of G-based ion intensities.

Whole biomass gel state ^{1}H-^{13}C HSQC

Heteronuclear Single Quantum Coherence (HSQC) NMR spectra were acquired for ball milled whole biomass samples (30–50 mg) dissolved in 500 µL DMSO-d6 and pyridine-d5 (4:1, 500 µL). Spectra were acquired at 40 °C on a Bruker Avance III 600 MHz spectrometer at 11.7 T using a room temperature broadband probe. Spectra were acquired with 1024 points and a SW of 12 ppm in the F2 (^{1}H) dimension and 256 points and SW of 220 ppm in the F1 (^{13}C) dimension. The spectral processing parameters from Mansfield et al. [51] were used and integrations were performed using TopSpin 3.6.

Solid-state ^{13}C NMR

High-resolution, solid-state ^{13}C NMR spectra were collected at 4.7 T with cross-polarization (CP) and magic angle spinning (MAS) in a Bruker Avance 200 MHz spectrometer. Interrupted decoupling spectra were obtained with 2.0 msec of variable amplitude CP to minimize intensity variations of the non-protonated aromatic carbons that are sensitive to Hartmann-Hahn mismatch at higher MAS rotation rates [82]. ^{1}H and ^{13}C fields were matched at 53.6 kHz and a 1 dB ramp was applied to the proton r.f. during the matching period. Proton decoupling began 30 µsec after the conclusion of CP. Simultaneous 90-degree refocusing pulses were applied to both nuclei to refocus any evolution caused by chemical shift interaction. This removed baseline distortions due to phasing errors. An additional 30 µsec delay for interrupted decoupling and refocusing was then applied. Acquisition time was 0.026 seconds with a spectral width of 20 kHz. MAS was performed at 6900 Hz with 40,000 scans averaged using a pulse repetition rate of 1.0 second. All ^{13}C chemical shifts were referenced externally to TMS at 0.0 ppm by setting the downfield resonance of Adamantane to 38.48 ppm. To calculate solid-state ^{13}C NMR S/G ratios for the poplar samples, the standard pine spectrum was scaled until the intensity of the shoulder at

148 ppm was equal to the intensity of the 148 ppm shoulder in the hardwood spectrum as described by Manders [56]. The softwood spectrum was then subtracted from the poplar spectrum and the result, theoretically, is a pure S spectrum. The S spectrum is then integrated from 158 ppm to 126 ppm and calibrated against the softwood spectrum which was integrated in the same manner and calibrated to 100. The G component was calculated by multiplying the softwood integration by the scaling factor from the subtraction. These values are then normalized to an equal number of unprotonated units on the benzene ring (divide S intensity by 4, divide G intensity by 3) before calculating the S/G ratio. We assume that intensity arising from 5–5 linkages has a negligible interference with the S/G ratio calculation due to their low abundance, 5% or less, in hardwood lignin [21, 56]. Spectral deconvolution of CP-MAS data was informed by extracting ^{13}C chemical shifts and linewidths from two-dimensional (2D) ^{13}C-^{13}C Dipolar Assisted Rotational Resonance (DARR) data on ^{13}C-enriched hardwood (DN34 Poplar) and softwood (Monterey Pine, IsoLife) samples [83].

Declarations

Funding

Author Contributions

RMH performed experiments, wrote text and edited manuscript, BA performed experiments wrote text and edited manuscript, CD performed experiments and prepared samples, BSD provided biomass wrote text and edited manuscript, MFD provided oversight and experimental design, AEW performed experiments, wrote text, edited manuscript and provided oversight

Acknowledgements

Data Availability: The Department of Energy will provide public access to these results of federally sponsored research in accordance with the DOE Public Access Plan(http://energy.gov/downloads/doe-public-access-plan). Data is available in the manuscript and any data not provided is available upon request from the coauthors.

Ethics approval and consent to participate: Not applicable

Consent for publication: Not applicable

Competing Interests: The authors declare no competing interests

References

1. Boerjan W, Ralph J, Baucher M. Lignin biosynthesis. Annu Rev Plant Biol. 2003;54:519-46.
2. Lee KH, Singh AP, Park BD, Wi SG, Bae HJ. Variability in the distribution of middle Lamella Lignin in secondary vascular tissues of kenaf stems. IAWA Journal. 2014;35(1):61-8.
3. Sykes R, Kodrzycki B, Tuskan G, Foutz K, Davis M. Within tree variability of lignin composition in Populus. Wood science and technology. 2008;42(8):649-61.
4. del Río JC, Rencoret J, Gutiérrez A, Elder T, Kim H, Ralph J. Lignin Monomers from beyond the Canonical Monolignol Biosynthetic Pathway: Another Brick in the Wall. ACS Sustainable Chemistry & Engineering. 2020;8(13):4997-5012.
5. Beckham GT, Johnson CW, Karp EM, Salvachúa D, Vardon DR. Opportunities and challenges in biological lignin valorization. Current Opinion in Biotechnology. 2016;42:40-53.
6. Davison BH, Parks J, Davis MF, Donohoe BS. Plant Cell Walls: Basics of Structure, Chemistry, Accessibility and the Influence on Conversion. Aqueous Pretreatment of Plant Biomass for Biological and Chemical Conversion to Fuels and Chemicals: Wiley; 2013. p. 23-38.
7. Chang H, Sarkanen V. Species Variation in Lignin: Effect of Species on the Rate of Kraft Delignification. Tappi J. 1973;56:132-4.
8. Magaton AD, Colodette JL, Gouvea ADG, Gomide JL, Muguet MCD, Pedrazzi C. Eucalyptus wood quality and its impact on kraft pulp production and use. Tappi J. 2009;8(8):32-9.
9. Huntley SK, Ellis D, Gilbert M, Chapple C, Mansfield SD. Significant Increases in Pulping Efficiency in C4H-F5H-Transformed Poplars: Improved Chemical Savings and Reduced Environmental Toxins. J Agric Food Chem. 2003;51(21):6178-83.
10. Tsutsumi Y, Kondo R, Sakai K, Imamura H. The difference of reactivity between syringyl lignin and guaiacyl lignin in alkaline systems. Holzforschung. 1995;49(5):423-8.
11. Chiang VL, Puumala RJ, Takeuchi H, Eckert RE. Comparison of Softwood and Hardwood Kraft Pulping. Tappi J. 1988;71(9):173-6.
12. Studer MH, DeMartini JD, Davis MF, Sykes RW, Davison B, Keller M, et al. Lignin content in natural Populus variants affects sugar release. Proceedings of the National Academy of Sciences.

2011;108(15):6300-5.

13. Davison BH, Drescher SR, Tuskan GA, Davis MF, Nghiem NP. Variation of S/G ratio and lignin content in a Populus family influences the release of xylose by dilute acid hydrolysis. Appl Biochem Biotechnol. 2006;130(1-3):427-35.

14. Ohlsson JA, Hallingbäck HR, Jebrane M, Harman-Ware AE, Shollenberger T, Decker SR, et al. Genetic variation of biomass recalcitrance in a natural Salix viminalis (L.) population. Biotechnology for Biofuels. 2019;12(1):135.

15. Ohlsson JA, Harman-Ware AE, Sandgren M, Schnürer A. Biomass Recalcitrance in Willow Under Two Biological Conversion Paradigms: Enzymatic Hydrolysis and Anaerobic Digestion. BioEnergy Research. 2019.

16. Wagner A, Tobimatsu Y, Phillips L, Flint H, Geddes B, Lu F, et al. Syringyl lignin production in conifers: Proof of concept in a Pine tracheary element system. Proceedings of the National Academy of Sciences. 2015;112(19):6218.

17. Rolando C, Monties B, Lapierre C. Thioacidolysis. In: Lin S, Dence C, editors. Methods in Lignin Chemistry. Springer Series in Wood Science: Springer Berlin Heidelberg; 1992. p. 334-49.

18. Harman-Ware AE, Foster C, Happs RM, Doeppke C, Meunier K, Gehan J, et al. Quantitative Analysis of Lignin Monomers by a Thioacidolysis Method Tailored for Higher-Throughput Analysis. Biotechnology Journal. 2016;11:1268-73.

19. Ralph J, Grabber JH. Dimeric ß-ether thioacidolysis products resulting from incomplete ether cleavage. Holzforschung. 1996;50(5):425-8.

20. Lapierre C, Pollet B, Monties B, Rolando C. Thioacidolysis of Spruce Lignin: GC-MS Analysis of the Main Dimers Recovered After Raney Nickel Desulphuration. Holzforschung. 1991;45(1):61-8.

21. Sjöström E. Lignin. Wood Chemistry: Fundamentals and Applications. 2nd Edition ed: Elsevier Science; 1993. p. 71-90.

22. Saito K, Watanabe Y, Shirakawa M, Matsushita Y, Imai T, Koike T, et al. Direct mapping of morphological distribution of syringyl and guaiacyl lignin in the xylem of maple by time-of-flight secondary ion mass spectrometry. Plant J. 2012;69(3):542-52.

23. Lapierre C. Application of new methods for the investigation of lignin structure. In: Jung HG, Bux- ton DR, Hatfield RD, Ralph J, editors. Forage Cell Wall Structure and Digestibility. Madison, WI: American Society of Agronomy; 1993. p. 133-66.

24. Li M, Foster C, Kelkar S, Pu Y, Holmes D, Ragauskas A, et al. Structural characterization of alkaline hydrogen peroxide pretreated grasses exhibiting diverse lignin phenotypes. Biotechnol Biofuels. 2012;5(1):38.

25. Grabber JH, Quideau S, Ralph J. p-coumaroylated syringyl units in maize lignin: Implications for β-ether cleavage by thioacidolysis. Phytochemistry. 1996;43:1189-94.

26. Ibarra D, Chávez MI, Rencoret J, Del Río JC, Gutiérrez A, Romero J, et al. Lignin Modification during Eucalyptus globulus Kraft Pulping Followed by Totally Chlorine-Free Bleaching: A Two-Dimensional

Nuclear Magnetic Resonance, Fourier Transform Infrared, and Pyrolysis – Gas Chromatography/Mass Spectrometry Study. J Agric Food Chem. 2007;55:3477-90.

27. Sarkanen KV, Hergert HL. Classification and distribution. In: Sarkanen KV, Ludwig CH, editors. Lignins: Occurrence, formation, structure and reactions. New York: Wiley-Interscience; 1971. p. 43-94.

28. Anderson EM, Stone ML, Katahira R, Reed M, Muchero W, Ramirez KJ, et al. Differences in S/G ratio in natural poplar variants do not predict catalytic depolymerization monomer yields. Nat Commun. 2019;10(1):2033.

29. Yokoi H, Ishida Y, Ohtani H, Tsuge S, Sonoda T, Ona T. Characterization of within-tree variation of lignin components in Eucalyptus camaldulensis by pyrolysis-gas chromatography. Analyst. 1999;124(5):669-74.

30. Rodrigues J, Meier D, Faix O, Pereira H. Determination of tree-to-tree variation in syringyl/guaiacyl ratio of Eucalyptus globulus wood lignin by analytical pyrolysis. Journal of Analytical and Applied Pyrolysis. 1999;48(2):121-8.

31. Rodrigues J, Graça J, Pereira H. Influence of tree eccentric growth on syringyl/guaiacyl ratio in Eucalyptus globulus wood lignin assessed by analytical pyrolysis. Journal of Analytical and Applied Pyrolysis. 2001;58–59(0):481-9.

32. Evtuguin DV, Neto CP, Silva AM, Domingues PM, Amado FM, Robert D, et al. Comprehensive study on the chemical structure of dioxane lignin from plantation Eucalyptus globulus wood. J Agric Food Chem. 2001;49(9):4252-61.

33. Asmadi M, Kawamoto H, Saka S. The effects of combining guaiacol and syringol on their pyrolysis. Holzforschung. 2012;66(3):323-30.

34. Izumi A, Kuroda K-i. Pyrolysis-mass spectrometry analysis of dehydrogenation lignin polymers with various syringyl/guaiacyl ratios. Rapid Communications in Mass Spectrometry. 1997;11(15):1709-15.

35. Decker SR, Harman-Ware AE, Happs RM, Wolfrum EJ, Tuskan GA, Kainer D, et al. High Throughput Screening Technologies in Biomass Characterization. Frontiers in Energy Research. 2018;6.

36. Harman-Ware AE, Macaya-Sanz D, Abeyratne CR, Doepkke C, Haiby K, Tuskan GA, et al. Accurate Determination of Genotypic Variance of Cell Wall Characteristics of a Populus trichocarpa Pedigree Using High-Throughput Pyrolysis-Molecular Beam Mass Spectrometry. Biotechnology for Biofuels. 2020.

37. Sykes R, Yung M, Novaes E, Kirst M, Peter G, Davis M. High-Throughput Screening of Plant Cell-Wall Composition Using Pyrolysis Molecular Beam Mass Spectroscopy. In: Mielenz JR, editor. Biofuels: Methods and Protocols. Totowa, NJ: Humana Press; 2009. p. 169-83.

38. Penning BW, Sykes RW, Babcock NC, Dugard CK, Klimek JF, Gamblin D, et al. Validation of PyMBMS as a High-throughput Screen for Lignin Abundance in Lignocellulosic Biomass of Grasses. BioEnergy Research. 2014;7(3):899-908.

39. Decker SR, Sykes RW, Turner GB, Lupoi JS, Doepkke C, Tucker MP, et al. High-throughput Screening of Recalcitrance Variations in Lignocellulosic Biomass: Total Lignin, Lignin Monomers, and Enzymatic

Sugar Release. JoVE. 2015(103):e53163.

40. Choi J-W, Faix O, Meier D. Characterization of Residual Lignins from Chemical Pulps of Spruce (*Picea abies L.*) and Beech (*Fagus sylvatica L.*) by Analytical Pyrolysis−Gas Chromatography/Mass Spectrometry. Holzforschung. 2001;55(2):185-92.

41. Genuit W, Boon JJ, Faix O. Characterization of beech milled wood lignin by pyrolysis-gas chromatography-photoionization mass spectrometry. Anal Chem. 1987;59(3):508-13.

42. Pu Y, Hallac B, Ragauskas AJ. Plant Biomass Characterization: Application of Solution and Solid-state NMR Spectroscopy. In: Wyman CE, editor. Aqueous Pretreatment of Plant Biomass for Biological and Chemical Conversion to Fuels and Chemicals. First ed. United Kingdom: John Wiley & Sons, Ltd.; 2013. p. 369-90.

43. Ralph J, Marita JM, Ralph SA, Hatfield RD, Lu F, Ede RM, et al. Solution state NMR of lignins. In: Argyropoulos DS, editor. Advances in Lignocellulosics Characterization. Atlanta, GA: Tappi Press; 1999. p. 55-108.

44. Granata A, Argyropoulos DS. 2-Chloro-4,4,5,5-tetramethyl-1,3,2-dioxaphospholane, a Reagent for the Accurate Determination of the Uncondensed and Condensed Phenolic Moieties in Lignins. J Agric Food Chem. 1995;43(6):1538-44.

45. Faix O, Argyropoulos D, Robert D, Neirinck V. Determination of Hydroxyl Groups in Lignins Evaluation of ^{1}H-, ^{13}C-, ^{31}P-NMR, FTIR and Wet Chemical Methods. Holzforschung. 1994;48(5):387-94.

46. Meng X, Crestini C, Ben H, Hao N, Pu Y, Ragauskas AJ, et al. Determination of hydroxyl groups in biorefinery resources via quantitative ^{31}P NMR spectroscopy. Nature Protocols. 2019;14(9):2627-47.

47. Argyropoulos DS. Heteronuclear NMR Spectroscopy of Lignins. In: Heitner C, Dimmel D, Schmidt J, editors. Lignin & Lignans; Advances in Chemistry. Boca Raton, FL: CRC Press; 2010. p. 245-65.

48. Heikkinen S, Toikka MM, Karhunen PT, Kilpeläinen IA. Quantitative 2D HSQC (Q-HSQC) via Suppression of J-Dependence of Polarization Transfer in NMR Spectroscopy: Application to Wood Lignin. Journal of the American Chemical Society. 2003;125(14):4362-7.

49. Lu F, Ralph J. Non-degradative dissolution and acetylation of ball-milled plant cell walls: high-resolution solution-state NMR. The Plant Journal. 2003;35(4):535-44.

50. Ralph J, Lu F. Cryoprobe 3D NMR of acetylated ball-milled pine cell walls. Organic & Biomolecular Chemistry. 2004;2(19):2714-5.

51. Mansfield SD, Kim H, Lu F, Ralph J. Whole plant cell wall characterization using solution-state 2D NMR. Nat Protoc. 2012;7(9):1579-89.

52. Capanema EA, Balakshin MY, Kadla JF. Quantitative Characterization of a Hardwood Milled Wood Lignin by Nuclear Magnetic Resonance Spectroscopy. Journal of Agricultural and Food Chemistry. 2005;53(25):9639-49.

53. Cheng K, Sorek H, Zimmermann H, Wemmer DE, Pauly M. Solution-State 2D NMR Spectroscopy of Plant Cell Walls Enabled by a Dimethylsulfoxide-d$_6$/1-Ethyl-3-methylimidazolium Acetate Solvent. Analytical Chemistry. 2013;85(6):3213-21.

54. Villaverde JJ, Li J, Ek M, Ligero P, de Vega A. Native Lignin Structure of Miscanthus x giganteus and Its Changes during Acetic and Formic Acid Fractionation. Journal of Agricultural and Food Chemistry. 2009;57(14):6262-70.

55. Talebi Amiri M, Bertella S, Questell-Santiago YM, Luterbacher JS. Establishing lignin structure-upgradeability relationships using quantitative ^{1}H–^{13}C heteronuclear single quantum coherence nuclear magnetic resonance (HSQC-NMR) spectroscopy. Chemical Science. 2019;10(35):8135-42.

56. Manders WF. Solid-state ^{13}C NMR determination of the syringyl/guaiacyl ratio in hardwoods. Holzforschung. 1987;41(1):13-8.

57. González-Vila FJ, Almendros G, del Rio JC, Martín F, Gutiérrez A, Romero J. Ease of delignification assessment of wood from different Eucalyptus species by pyrolysis (TMAH)-GC/MS and CP/MAS ^{13}C-NMR spectrometry. Journal of Analytical and Applied Pyrolysis. 1999;49(1):295-305.

58. Martínez AT, González AE, Valmaseda M, Dale BE, Lambregts MJ, Haw JF. Solid-state NMR studies of lignin and plant polysaccharide degradation by fungi. Holzforschung-International Journal of the Biology, Chemistry, Physics and Technology of Wood. 1991;45(s1):49-54.

59. Hawkes GE, Smith CZ, Utley JHP, Vargas RR, Viertler H. A comparison of solution and solid state ^{13}C NMR spectra of lignins and lignin model compounds. Holzforschung-International Journal of the Biology, Chemistry, Physics and Technology of Wood. 1993;47(4):302-12.

60. Fidalgo ML, Terron MC, Martinez AT, Gonzalez AE, Gonzalez-Vila FJ, Galletti GC. Comparative study of fractions from alkaline extraction of wheat straw through chemical degradation, analytical pyrolysis, and spectroscopic techniques. Journal of Agricultural and Food Chemistry. 1993;41(10):1621-6.

61. Martınez AT, Almendros G, González-Vila FJ, Fründ R. Solid-state spectroscopic analysis of lignins from several Austral hardwoods. Solid state nuclear magnetic resonance. 1999;15(1):41-8.

62. Newman RH, Tauwhare SEK, Scheele S, Te Kanawa R. Leaf-fiber lignins of Phormium varieties compared bysolid-state ^{13}C NMR spectroscopy. Holzforschung. 2005;59(2):147-52.

63. Foston M, Hubbell CA, Samuel R, Jung S, Fan H, Ding S-Y, et al. Chemical, ultrastructural and supramolecular analysis of tension wood in Populus tremula x alba as a model substrate for reduced recalcitrance. Energy & Environmental Science. 2011;4(12):4962-71.

64. Davis MF, Schroeder HR, Maciel GE. Solid-state ^{13}C nuclear magnetic resonance studies of wood decay. I. White rot decay of Colorado blue spruce. Walter de Gruyter, Berlin/New York; 1994.

65. Davis MF, Schroeder HA, Maciel GE. Solid-State ^{13}CNuclear Magnetic Resonance Studies of Wood Decay. II. White Rot Decay of Paper Birch. Holzforschung-International Journal of the Biology, Chemistry, Physics and Technology of Wood. 1994;48(3):186-92.

66. Kang X, Kirui A, Dickwella Widanage MC, Mentink-Vigier F, Cosgrove DJ, Wang T. Lignin-polysaccharide interactions in plant secondary cell walls revealed by solid-state NMR. Nature Communications. 2019;10(1):347.

67. Harman-Ware AE, Happs RM, Davison BH, Davis MF. The effect of coumaryl alcohol incorporation on the structure and composition of lignin dehydrogenation polymers. Biotechnology for Biofuels. 2017;10(1):281.

68. Addison B, Onofrei D, Stengel D, Blass B, Brenneman B, Ayon J, et al. Spider prey-wrapping silk is an α-helical coiled-coil/β-sheet hybrid nanofiber. Chemical Communications. 2018;54(76):10746-9.

69. Domján A, Bajdik J, Pintye-Hódi K. Understanding of the Plasticizing Effects of Glycerol and PEG 400 on Chitosan Films Using Solid-State NMR Spectroscopy. Macromolecules. 2009;42(13):4667-73.

70. Fergus BJ, Goring DAI. The Distribution of Lignin in Birch Wood as Determined by Ultraviolet Microscopy. Holzforschung. 1970;24(4):118.

71. Donaldson LA. Lignification and lignin topochemistry - an ultrastructural view. Phytochemistry. 2001;57(6):859-73.

72. Mehring M. Principles of High Resolution NMR in Solids. New York: Springer-Verlag; 1983. 356 p.

73. Kolodziejski W, Klinowski J. Kinetics of cross-polarization in solid-state NMR: A guide for chemists. Chemical Reviews. 2002;102(3):613-28.

74. Pu Y, Hallac B, Ragauskas AJ. Plant Biomass Characterization: Application of Solution- and Solid-State NMR Spectroscopy. In: Wyman CE, editor. Aqueous Pretreatment of Plant Biomass for Biological and Chemical Conversion to Fuels and Chemicals. Chichester, UK: John Wiley & Sons, Ltd; 2013. p. 369-90.

75. Li Y, Akiyama T, Yokoyama T, Matsumoto Y. NMR Assignment for Diaryl Ether Structures (4−O−5 Structures) in Pine Wood Lignin. Biomacromolecules. 2016;17(6):1921-9.

76. Yue F, Lu F, Ralph S, Ralph J. Identification of 4−O−5-Units in Softwood Lignins via Definitive Lignin Models and NMR. Biomacromolecules. 2016;17(6):1909-20.

77. Aoki D, Nomura K, Hashiura M, Imamura Y, Miyata S, Terashima N, et al. Evaluation of ring-5 structures of guaiacyl lignin in Ginkgo biloba L. using solid- and liquid-state ^{13}C NMR difference spectroscopy. Holzforschung. 2019;73(12):1083-92.

78. Gao X, Laskar DD, Zeng J, Helms GL, Chen S. A ^{13}C CP/MAS-Based Nondegradative Method for Lignin Content Analysis. ACS Sustainable Chemistry & Engineering. 2015;3(1):153-62.

79. Sparrman T, Svenningsson L, Sahlin-Sjövold K, Nordstierna L, Westman G, Bernin D. A revised solid-state NMR method to assess the crystallinity of cellulose. Cellulose. 2019;26(17):8993-9003.

80. Park S, Johnson DK, Ishizawa CI, Parilla PA, Davis MF. Measuring the crystallinity index of cellulose by solid state ^{13}C nuclear magnetic resonance. Cellulose. 2009;16(4):641-7.

81. Yue F, Lu F, Sun R-C, Ralph J. Syntheses of Lignin-Derived Thioacidolysis Monomers and Their Uses as Quantitation Standards. Journal of Agricultural and Food Chemistry. 2012;60(4):922-8.

82. Peersen OB, Wu XL, Kustanovich I, Smith SO. Variable-amplitude cross-polarization MAS NMR. J Magn Reson. 1993;104(3):334-9.

83. Takegoshi K, Nakamura S, Terao T. ^{13}C−^{1}H dipolar-assisted rotational resonance in magic-angle spinning NMR. Chemical Physics Letters. 2001;344(5):631-7.
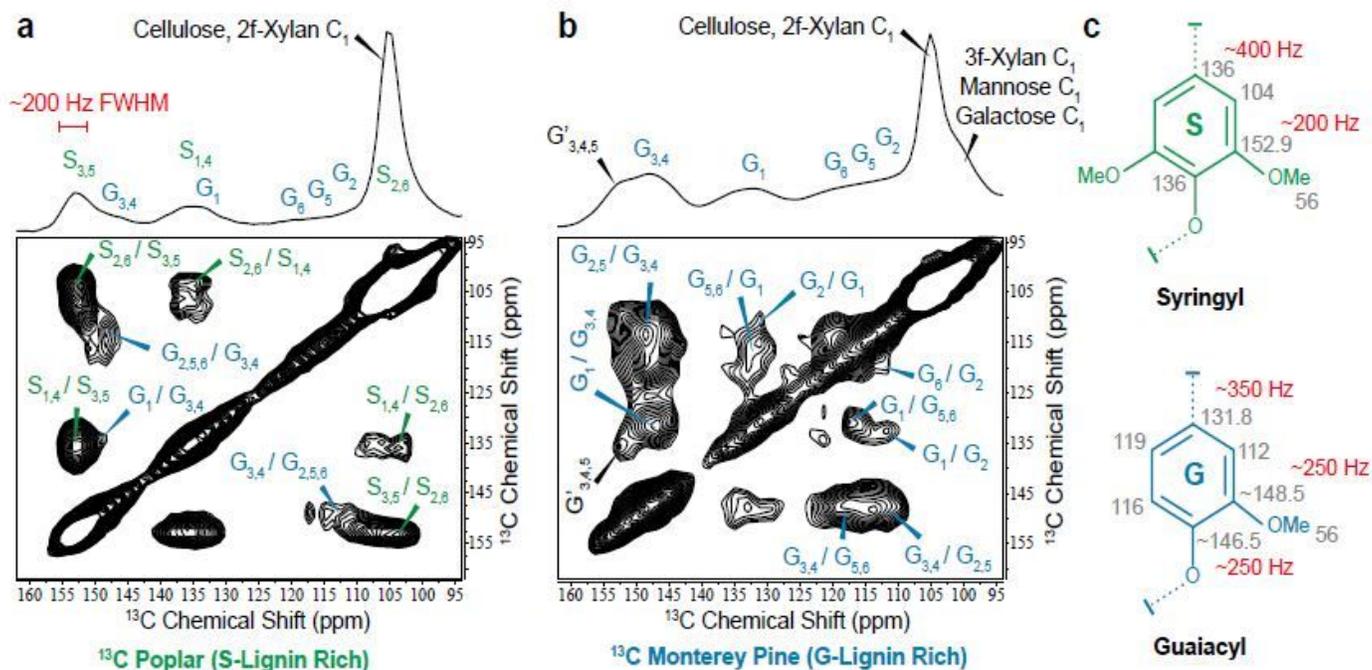
Figures

Figure 1

Aromatic region of through-space two-dimensional 13C-13C correlation data on (a) 13C-enriched poplar woody stems and (b) 13C-enriched Monterey pine. 13C chemical shifts and approximate linewidths were extracted from the data and listed in grey and red text next to monomeric chemical structures shown in (c).
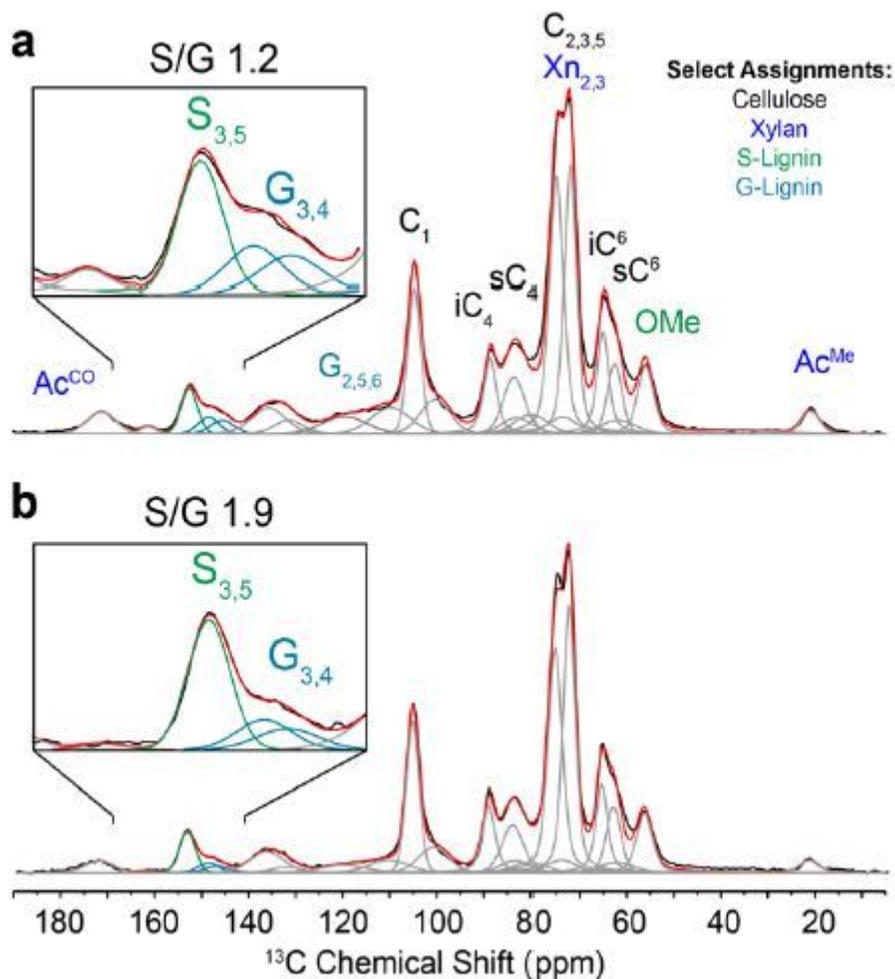
Figure 2

Example spectral deconvolution of 1H-13C CP-MAS data obtained from low-S (a) and high-S (b) natural poplar variants. Lignin S/G ratios were obtained from deconvoluted peak areas from lignin S3,5 and G3,4 signals located near 153 and 146-148 ppm, respectively.
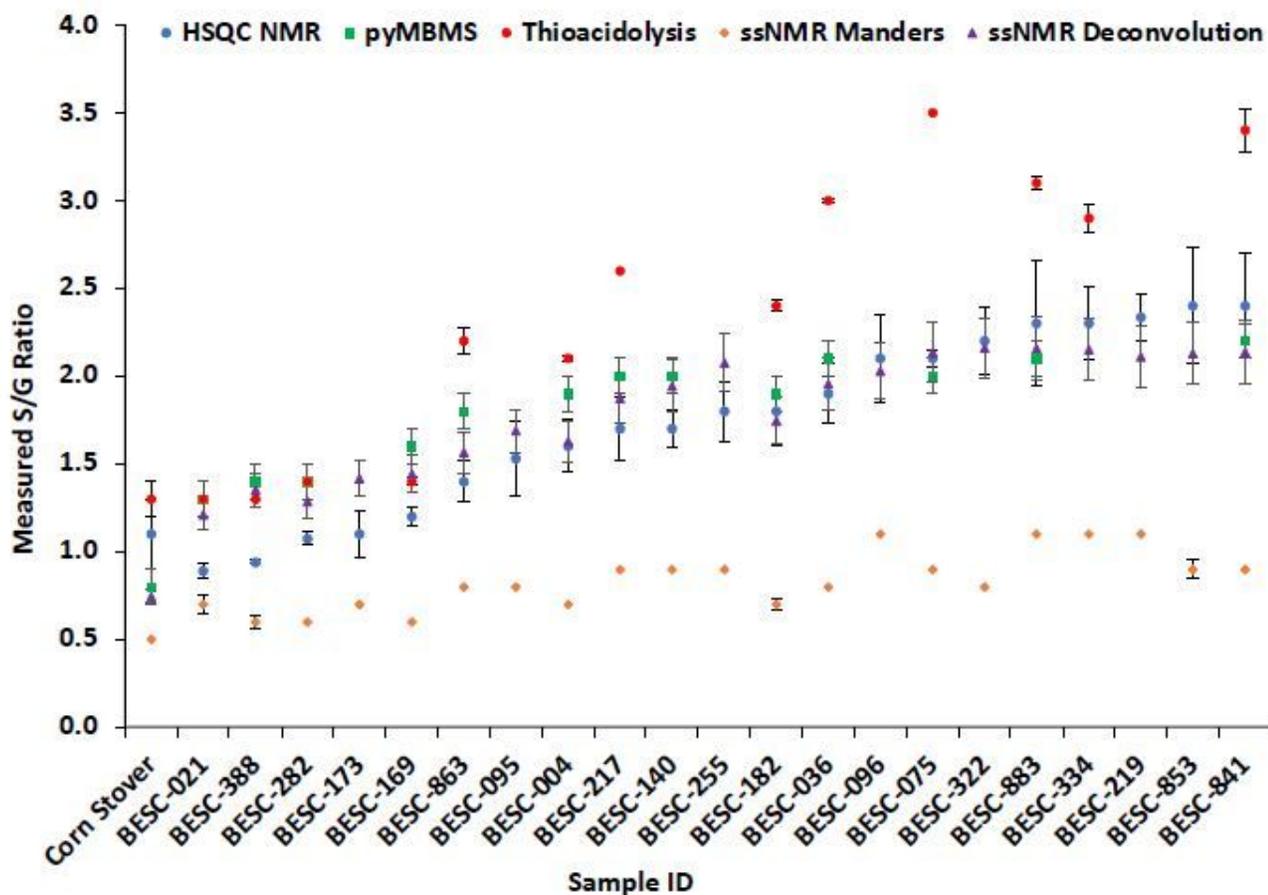
Figure 3

Comparison of S/G ratios in corn stover and poplar measured, calculated, and/or predicted by thioacidolysis, py-MBMS, HSQC, ssNMR Manders method, and ssNMR spectral deconvolution. Samples are sorted for graphical viewing by listing corn stover first, and sorting poplar samples via HSQC measured S/G ratios.

Supplementary Files

This is a list of supplementary files associated with this preprint. Click to download.

- SupplementalTable3final.xlsx
- SupplementalTable2final.xlsx
- SupplementalTable1final.xlsx